eLIFE
elifesciences.org

Figures and figure supplements

Mitochondrial Ca^{2+} uptake by the voltage-dependent anion channel 2 regulates cardiac rhythmicity

Hirohito Shimizu, et al.

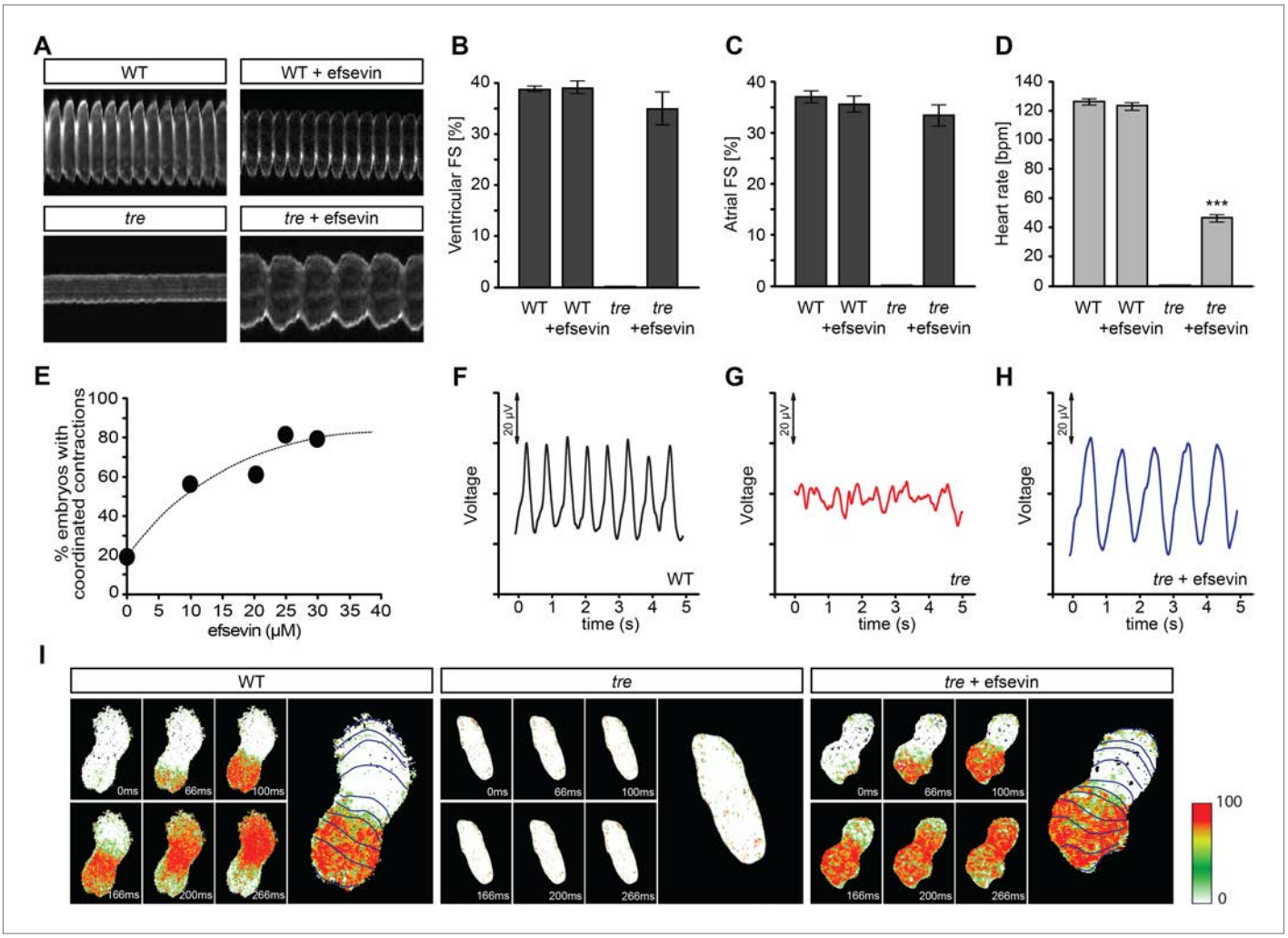

Figure 1. Efsevin restores rhythmic cardiac contractions in zebrafish tremblor embryos. (**A**) Line scans across the atria of *Tg(myl7:GFP)* embryonic hearts at 48 hpf. Rhythmically alternating systoles and diastoles are recorded from vehicle- (upper left) or efsevin- treated wild type (upper right) and efsevin-treated *tre* (lower right) embryos, while only sporadic unsynchronized contractions are recorded from vehicle-treated *tre* embryos (lower left). (**B**, **C**) Fractional shortening (FS) deduced from the line-scan traces. While cardiac contraction was not observed in *tre*, efsevin-treated wild type and *tre* hearts have similar levels of FS to those observed in control hearts. Ventricular FS of wild type v.s. wild type + efsevin vs tre + efsevin: 39 ± 0.6%, n = 8 vs 39 ± 1%, n = 10 vs 35 ± 3%, n = 6; and Atrial FS: 37 ± 1%, n = 11 vs 35 ± 2%, n = 11 vs 33 ± 2%, n = 15. (**D**) While efsevin restored a heart rate of 46 ± 2 beats per minute (bpm) in *tre* embryos, same treatment does not affect the heart rate in wild type embryos (126 ± 2 bpm in vehicle-treated embryos vs 123 ± 3 bpm in efsevin-treated wild-type embryos). ***, $p < 0.001$ by one-way ANOVA. (**E**) Dose-dependence curve for efsevin. The *tre* embryos were treated with various concentrations of efsevin from 24 hpf and cardiac contractions were analyzed at 48 hpf. (**F**–**H**) Representative time traces of local field potentials for wild type (**F**), *tre* (**G**) and efsevin-treated *tre* (**H**) embryos clearly display periods of regular, irregular, and restored periodic electrical activity. (**I**) In vivo optical maps of Ca^{2+} activation represented by isochronal lines every 33 ms recorded from 36 hpf wild type (left), *tre* (center) and efsevin-treated *tre* (right) embryos.

DOI: 10.7554/eLife.04801.003

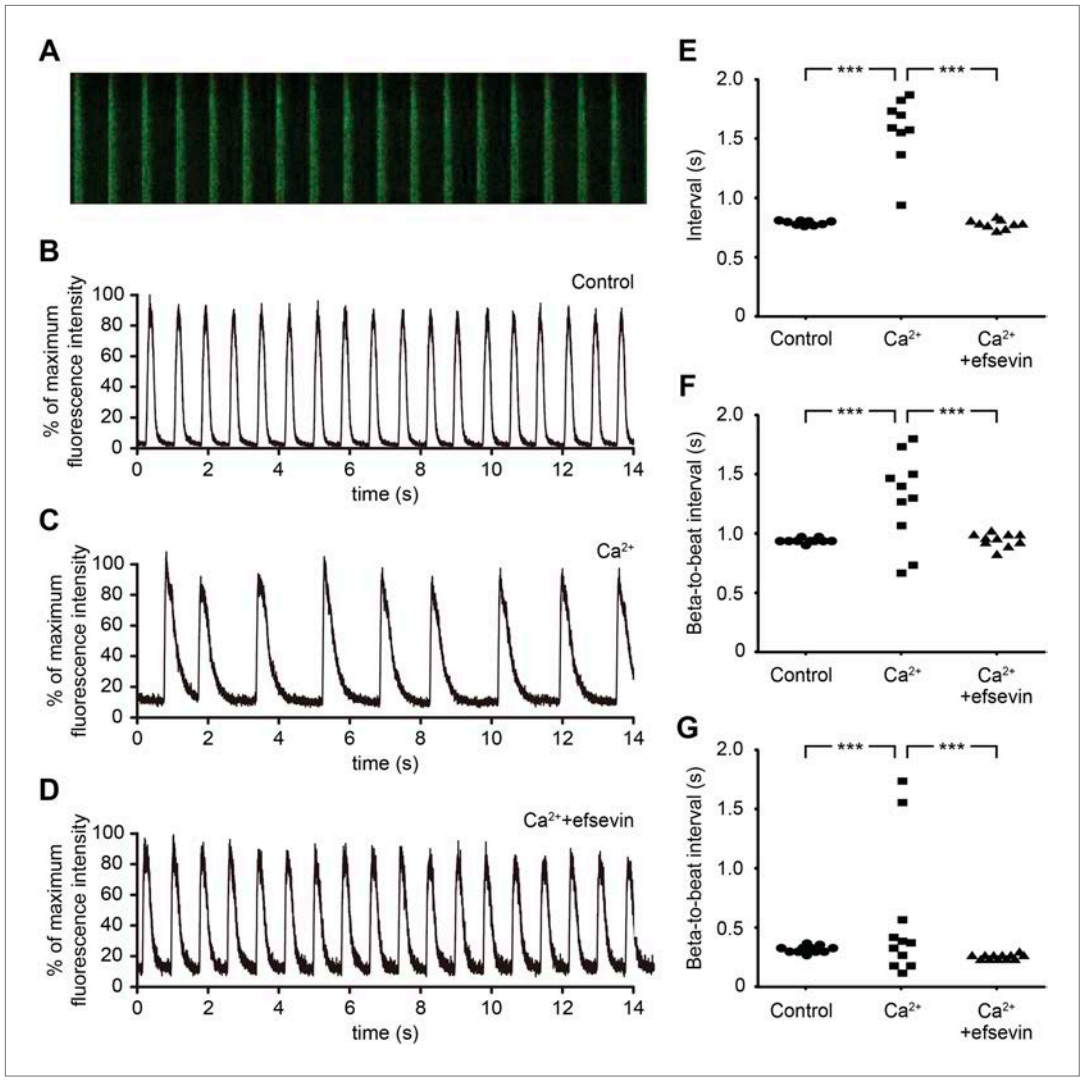

Figure 2. Efsevin reduces arrhythmogenic events in ES cell-derived cardiomyocytes. (**A**) Line-scan analysis of Ca^{2+} transients in mESC-CMs after 10 days of differentiation. (**B**–**D**) Representative graph of Ca^{2+} transients detected in mESC-CMs (**B**). After treatment with 10 mM Ca^{2+} for 10 min, the EB showed an irregular pattern of Ca^{2+} transients (**C**). Efsevin treatment restores regular Ca^{2+} transients under Ca^{2+} overload conditions in mESC-CMs (**D**). (**E**) Plotted intervals between peaks of Ca^{2+} signals detected in mESC-CMs prior to treatment (control), in 10 mM Ca^{2+}_{ext} (Ca^{2+}) and in 10 mM Ca^{2+}_{ext}+10 μM efsevin (Ca^{2+}+efsevin). (**F**, **G**) Plotted intervals of contractions detected in EBs prior to treatment (control), in 10 mM Ca^{2+}_{ext} (Ca^{2+}) and in 10 mM Ca^{2+}_{ext} + 10 μM efsevin (Ca^{2+} + efsevin) for mouse ESC-CMs (**F**) and 5 mM Ca^{2+}_{ext} (Ca^{2+}) and in 5 mM Ca^{2+}_{ext} + 5 μM efsevin (Ca^{2+} + efsevin) for human ESC-CMs (**G**). ***, $p < 0.001$ by F-test.

DOI: 10.7554/eLife.04801.011

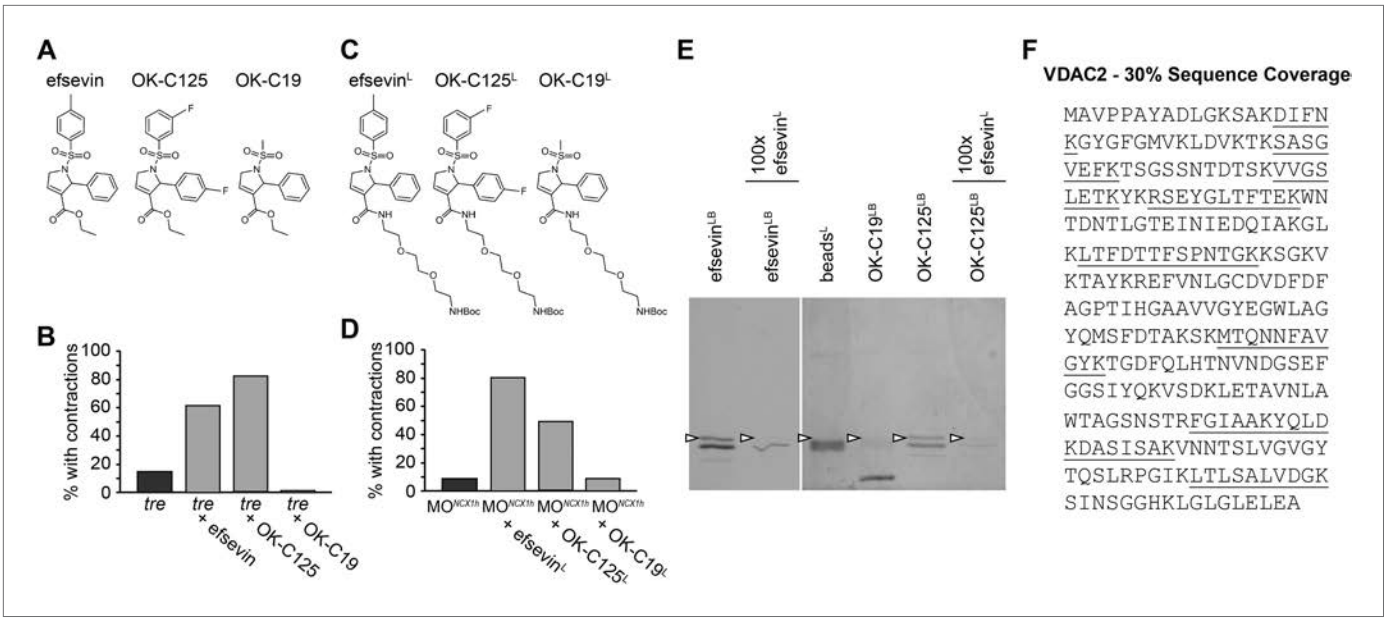

Figure 3. VDAC2 is a protein target of efsevin. (**A**) Structures of efsevin and two derivatives, OK-C125 and OK-C19. (**B**) Efsevin and OK-C125 restored rhythmic contractions in the majority of *tremblor* embryos, whereas OK-C19 failed to rescue the *tremblor* phenotype. (**C**) Structures of linker-attached compounds (indicated by superscript L). (**D**) Compounds efsevin^{L} and OK-C125^{L} retained their ability to restore rhythmic contractions in NCX1hMO injected embryos, while the inactive derivative OK-C19^{L} was still unable to induce rhythmic contraction. (**E**) Affinity agarose beads covalently linked with efsevin (efsevin^{LB}) or OK-C125 (OK-C125^{LB}) pulled down 2 protein species from zebrafish embryonic lysate, whereof one, the 32 kD upper band, was sensitive to competition with a 100-fold excess free efsevin^{L}. The 32 kD band was not detected in proteins eluted from beads capped with ethanolamine alone (beads^{C}) or beads linked to OK-C19 (OK-C19^{LB}). Arrowheads point to the 32kD bands. (**F**) Mass Spectrometry identifies the 32kD band as VDAC2. Peptides identified by mass spectrometry (underlined) account for 30% of the total sequence.

DOI: 10.7554/eLife.04801.012

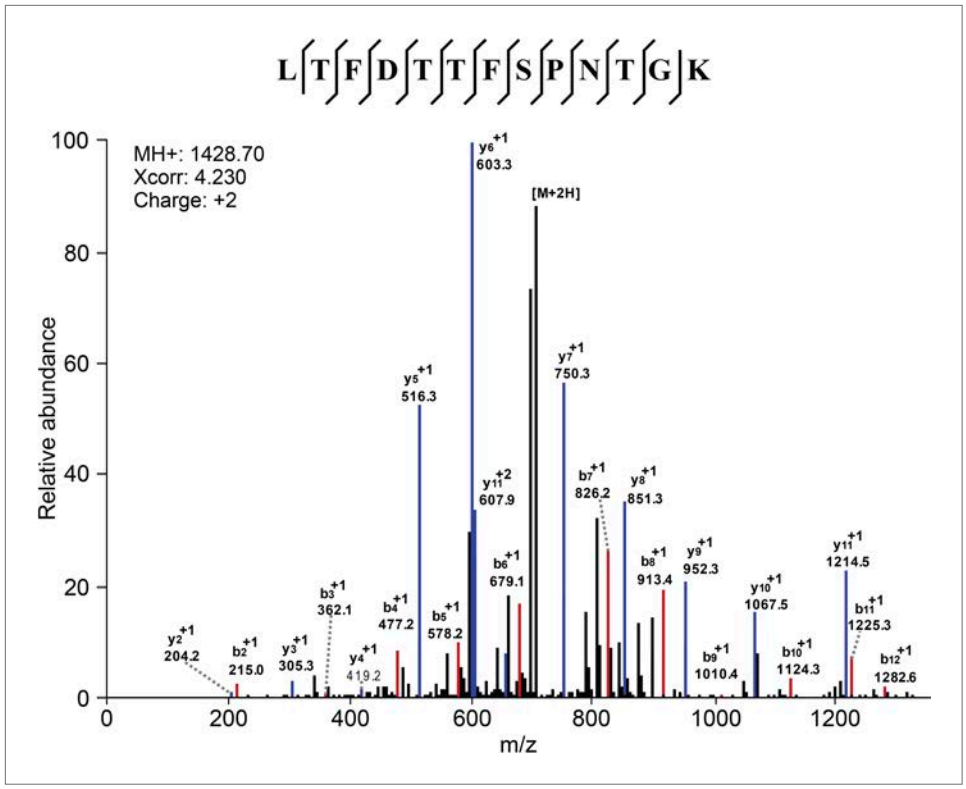

Figure 3—figure supplement 1. Mass Spectometry identifies VDAC2 as the target of efsevin. Image shows an example of the identification of VDAC2 peptide. Diagnostic b- and y-series ions are shown in red and blue, respectively.

DOI: 10.7554/eLife.04801.013

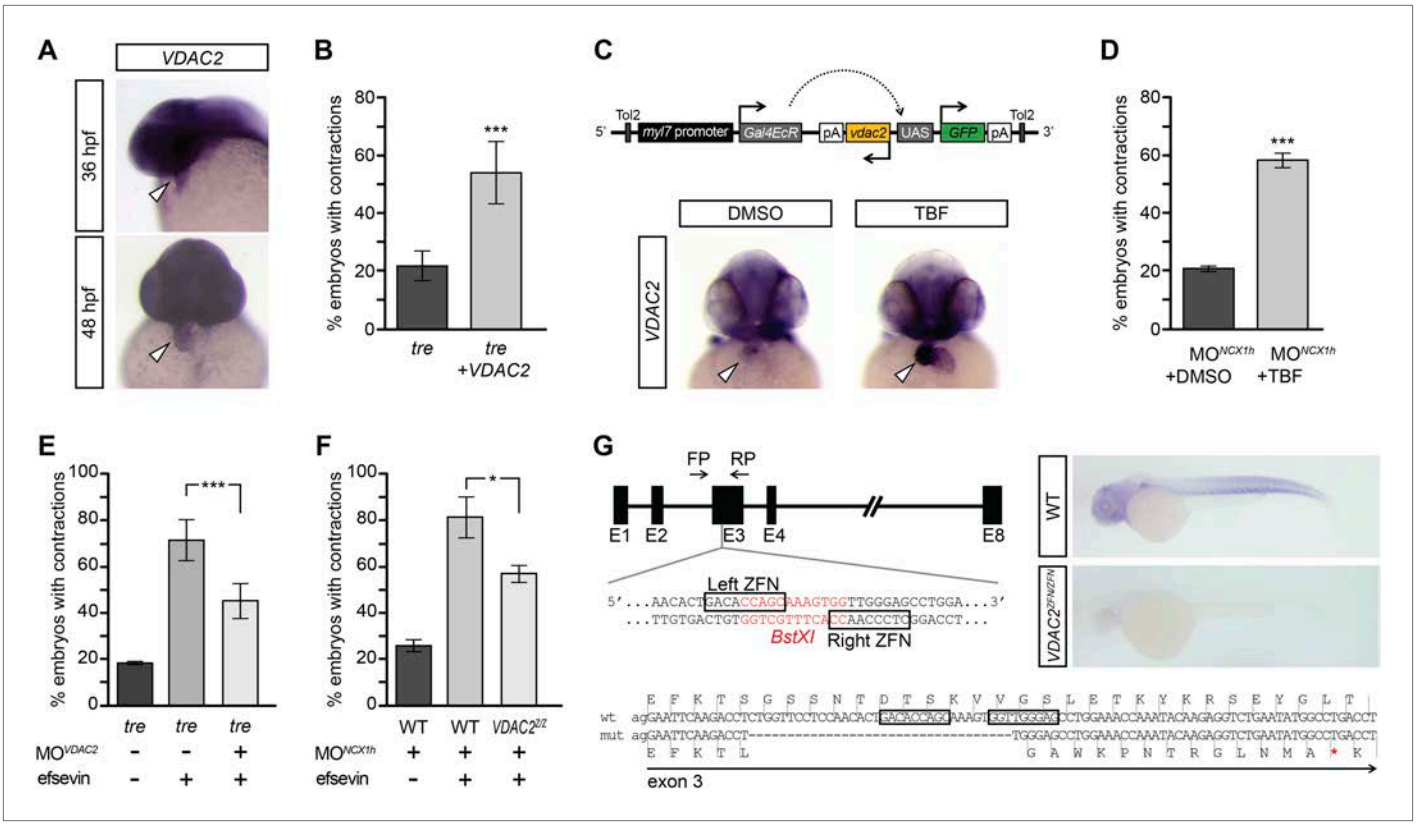

Figure 4. VDAC2 restores rhythmic cardiac contractions in *tre*. (**A**) In situ hybridization analysis showed that VDAC2 is expressed in embryonic hearts at 36 hpf (upper image) and 48 hpf (lower image). (**B**) Injection of 25 pg in vitro synthesized VDAC2 mRNA restored cardiac contractions in 52.9 ± 12.1% (n = 78) of 1-day-old *tre* embryos, compared to 21.8 ± 5.1% in uninjected siblings (n = 111). (**C**) Schematic diagram of *myl7:VDAC2* construct (top). In situ hybridization analysis showed that TBF treatment induces VDAC2 expression in the heart (lower panel). (**D**) While only ~20% of *myl7:VDAC2;NCX1hMO* embryos have coordinated contractions (n = 116), 52.3 ± 2.4% of these embryos established persistent, rhythmic contractions after TBF induction of VDAC2 (n = 154). (**E**) On average, 71.2 ± 8.8% efsevin treated embryos have coordinated cardiac contractions (n = 131). Morpholino antisense oligonucleotide knockdown of VDAC2 (MO^{VDAC2}) attenuates the ability of efsevin to suppress cardiac fibrillation in *tre* embryos (45.3 ± 7.4% embryos with coordinated contractions, n = 94). (**F**) Efsevin treatment restores coordinated cardiac contractions in 76.2 ± 8.7% NCX1MO embryos, only 54.1 ± 3.6% $VDAC2^{zfn/zfn}$;NCX1MO embryos have coordinated contractions (n = 250). (**G**) Diagram of Zinc finger target sites. $VDAC2^{zfn/zfn}$ carries a 34 bp deletion in exon 3 which results in a premature stop codon (red asterisk). In situ hybridization analysis showing loss of VDAC2 transcripts in $VDAC2^{zfn/zfn}$ embryos. White arrowheads point to the developing heart.

DOI: 10.7554/eLife.04801.014

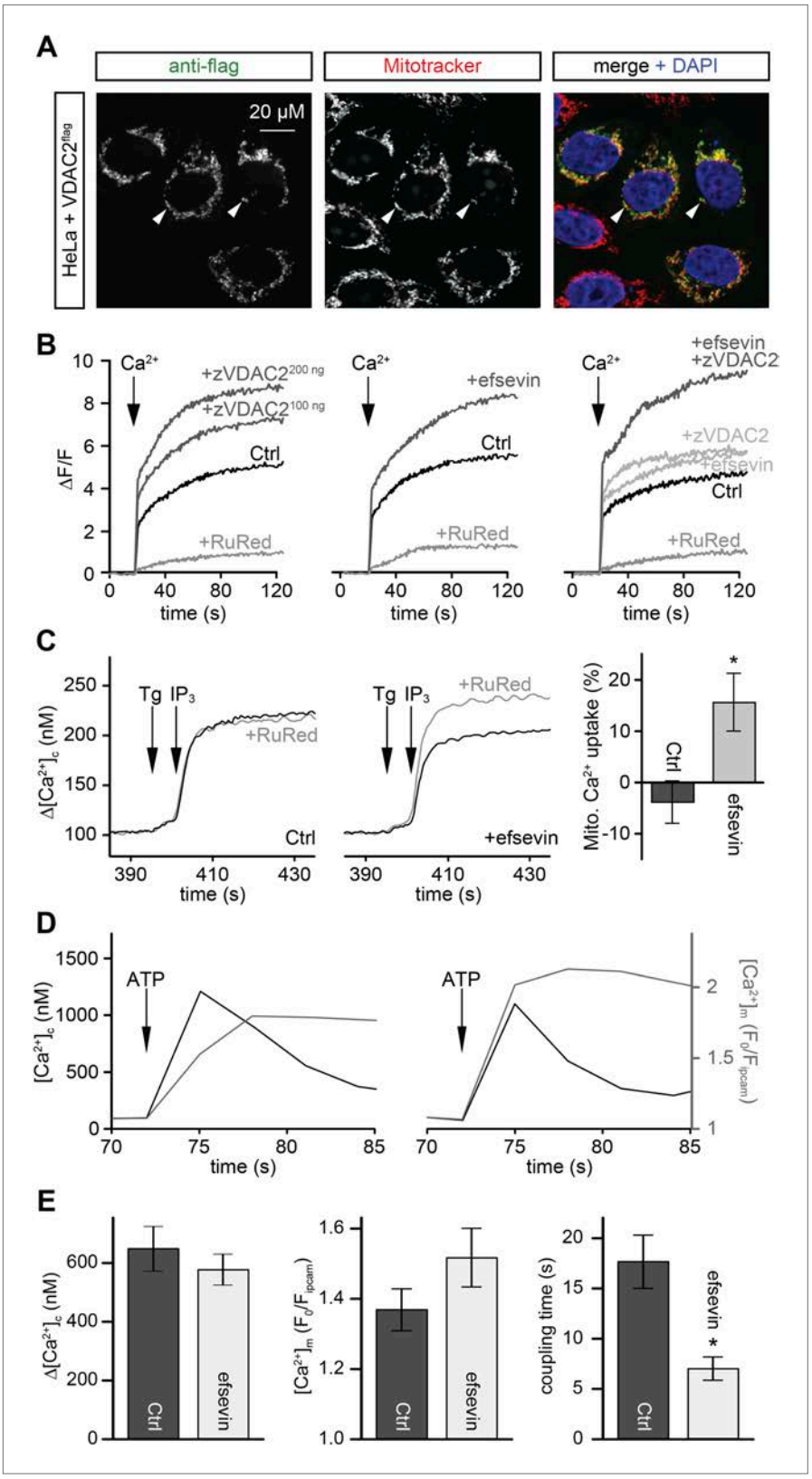

Figure 5. Efsevin enhances mitochondrial Ca^{2+} uptake. (**A**) HeLa cells were transfected with a flag-tagged zebrafish VDAC2 ($VDAC2^{flag}$), immunostained against the flag epitope and counterstained for mitochondria with MitoTracker Orange and for nuclei with DAPI. (**B**) Representative traces of mitochondrial matrix $[Ca^{2+}]$ ($[Ca^{2+}]_m$) detected by

Figure 5. Continued on next page

Figure 5. Continued

Rhod2. Arrows denote the addition of Ca^{2+}. Mitochondrial Ca^{2+} uptake was assessed when VDAC2 was overexpressed (left), cells were treated with 1 μM efsevin (middle) and combination of both at suboptimal doses (right). Control-traces with ruthenium red (RuRed) show mitochondrial specificity of the signal. (**C**) Representative traces of cytosolic [Ca^{2+}] ($[Ca^{2+}]_c$) changes upon the application of 7.5 μM IP_3 in the presence (+) or absence (−) of RuRed. Mitochondrial Ca^{2+} uptake was assessed by the difference of the – and + RuRed conditions normalized to the total release (n = 4; mean ± SE). (**D**) MEFs overexpressing zebrafish VDAC2 (polycistronic with mCherry) were stimulated with 1 μM ATP in a nominally Ca^{2+} free buffer. Changes in $[Ca^{2+}]_c$ and $[Ca^{2+}]_m$ were imaged using fura2 and mitochondria-targeted inverse pericam, respectively. Black and gray traces show the $[Ca^{2+}]_c$ (in nM) and $[Ca^{2+}]_m$ (F_0/F mtpericam) time courses in the absence (left) or present (right) of efsevin. (**E**) Bar charts: Cell population averages for the peak $[Ca^{2+}]_c$ (left), the corresponding $[Ca^{2+}]_m$ (middle), and the coupling time (time interval between the maximal $[Ca^{2+}]_c$ and $[Ca^{2+}]_m$ responses) in the presence (black, n = 24) or absence (gray, n = 28) of efsevin.

DOI: 10.7554/eLife.04801.024

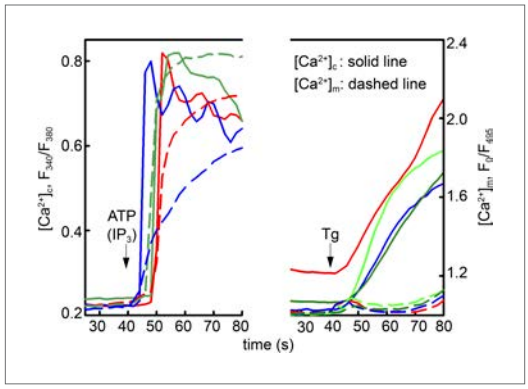

Figure 5—figure supplement 1. Local Ca^{2+} delivery between IP3 receptors and VDAC2. V1V3DKO MEFs were stimulated with 100 μM ATP (left) or 2 μM thapsigargan (Tg) (right). Changes in $[Ca^{2+}]_c$ and $[Ca^{2+}]_m$ were imaged using fura2 and mitochondria targeted inverse pericam, respectively. Representative traces obtained in three cells are shown.

DOI: 10.7554/eLife.04801.025

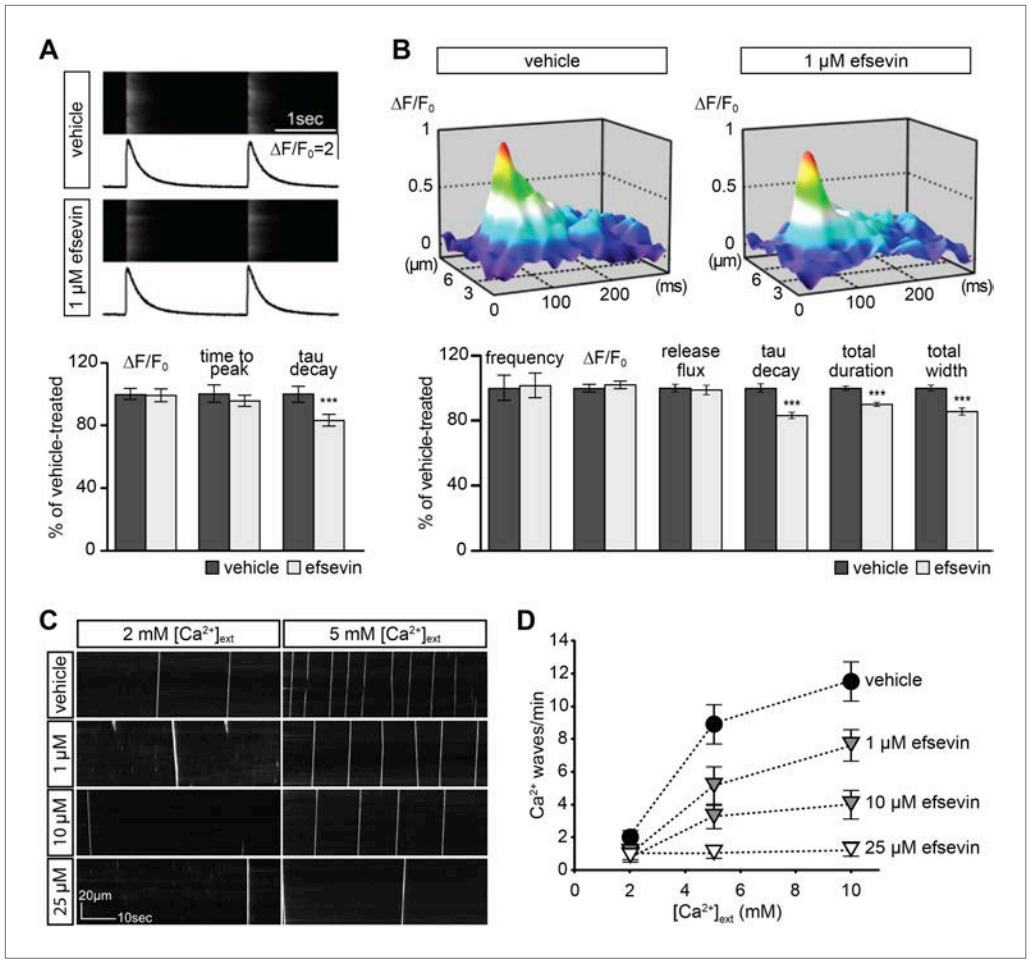

Figure 6. Effects of efsevin on isolated cardiomyocytes. (**A**) Electrically paced Ca^{2+} transients at 0.5 Hz (top). Normalized quantification of Ca^{2+} transient parameters reveals no difference for transient amplitude (efsevin-treated at 98.6 ± 4.5% of vehicle-treated) and time to peak (95 ± 3.9%), but a significant decrease for the rate of decay (82.8 ± 4% of vehicle- for efsevin-treated) (lower panel). (**B**) Representation of typical Ca^{2+} sparks of vehicle- and efsevin treated cardiomyocytes (top). No differences were observed for spark frequency (101.1 ± 7.7% for efsevin- compared to vehicle-treated), maximum spark amplitude (101.6 ± 2.5%) and Ca^{2+} release flux (98.7 ± 2.8%). In contrast, the decay phase of the single spark was significantly faster in efsevin treated cells (82.5 ± 2.1% of vehicle-treated). Consequently, total duration of the spark was reduced to 85.7 ± 2% and the total width was reduced to 89.5 ± 1.4% of vehicle-treated cells. *, $p < 0.05$; ***, $p < 0.001$. (**C**) Increasing concentrations of extracellular Ca^{2+} induced a higher frequency of spontaneous propagating Ca^{2+} waves in isolated adult murine ventricular cardiomyocytes. Efsevin treatment reduced Ca^{2+} waves in a dose-dependent manner. (**D**) Quantitative analysis of spontaneous Ca^{2+} waves spanning more than half of the entire cell. Addition of 1 μM efsevin reduced Ca^{2+} waves to approximately half. Increasing the concentration of efsevin to 10 μM further reduced the number of spontaneous Ca^{2+} waves and 25 μM efsevin almost entirely blocked the formation of Ca^{2+} waves.

DOI: 10.7554/eLife.04801.026

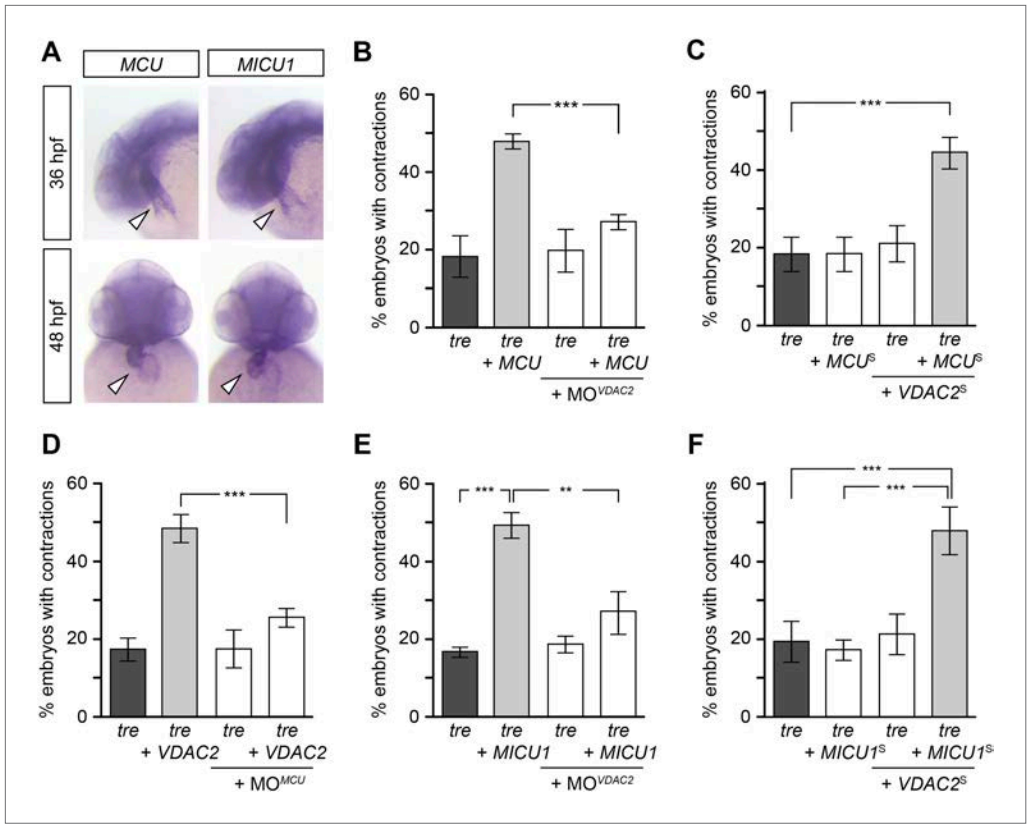

Figure 7. Mitochondria regulate cardiac rhythmicity through a VDAC2-dependent mechanism. (**A**) MCU and MICU1 are expressed in the developing zebrafish hearts (arrowhead). (**B**) Overexpression of MCU is sufficient to restore coordinated cardiac contractions in *tre* embryos (47.1 ± 1.6% embryos, n = 112 as opposed to 18.3 ± 5.3% of uninjected siblings, n = 64) while this effect is significantly attenuated when co-injected with morpholino antisense oligonucleotide targeted to VDAC2 (27.1 ± 1.9% embryos, n = 135). (**C**) Suboptimal overexpression of MCU (MCU^S) and VDAC2 ($VDAC2^S$) in combination is able to suppress cardiac fibrillation in *tre* embryos (42.9 ± 2.6% embryos, n = 129). (**D**) The ability of VDAC2 to restore rhythmic contractions in *tre* embryos (48.5 ± 3.5% embryos, n = 111) is significantly attenuated when MCU is knocked down by antisense oligonucleotide (MO^{MCU}) (25.6 ± 2.4% embryos, n = 115). (**E**) Overexpression of MICU1 is sufficient to restore rhythmic cardiac contractions in *tre* embryos (49.3 ± 3.4% embryos, n = 127 compared to 16.8 ± 1.4% of uninjected siblings, n = 150). This effect is abrogated by VDAC2 knockdown (MO^{VDAC2}, 25.3 ± 5.5% embryos, n = 97). (**F**) Suboptimal overexpression of MICU1 ($MICU1^S$) and VDAC2 ($VDAC2^S$) in combination is able to restore rhythmic cardiac contractions in *tre* embryos (48.6 ± 6.0%, n = 106). Error bars represent s.d.; *p < 0.05; ***p < 0.001.

DOI: 10.7554/eLife.04801.027

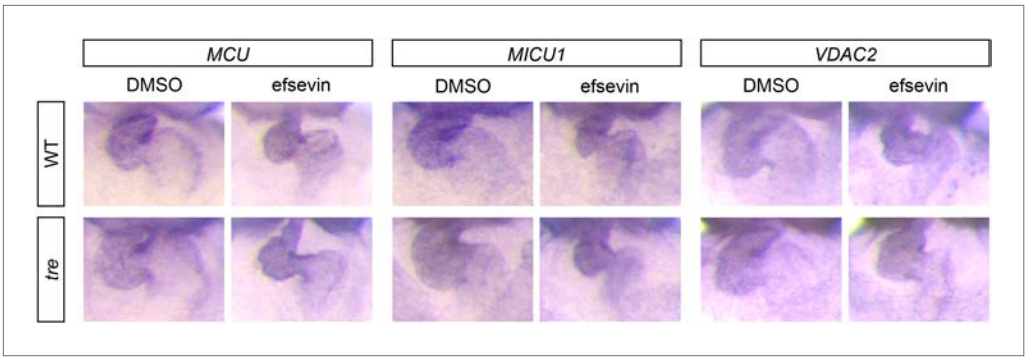

Figure 7—figure supplement 1. Expression of MCU, MICU1 and VDAC2. In situ hybridization analysis shows that the expression levels of MCU, MICU1 and VDAC2 are comparable between wild type and *tre* embryos with and without efsevin treatment.

DOI: 10.7554/eLife.04801.028